Melting temperature of iron in the core – diamond cell experiments

Guoyin Shen

Center for Advanced Radiation Sources
The University of Chicago
Chicago, USA
Email: shen@cars.uchicago.edu

Introduction

There are two major techniques commonly used for ultrahigh pressure melting studies: shock wave experiments and the internally heated diamond anvil cell (DAC). In shock compression experiments, the sample is subjected to high pressures and high temperatures by dynamic processes (see the section by ???Ahrens). In DAC experiments, pressure is generated by pressing two opposing diamond anvils, while heating is applied resistively and/or using laser heating. Both techniques have been extensively applied to study high pressure melting of iron. However, accurate determination of melting is exceedingly difficult at extremely high pressure and temperature conditions. The associated weaknesses - the short time scale in shock compression and the small sample size in DAC - are reflected by the large uncertainties and the discrepancy among literature values on melting temperature of iron in the core.

In this section, we begin with a brief description of the generation of simultaneous high pressures and temperatures in the DAC, followed by a discussion on the observation of the onset of the melting transition and the determination of pressure-temperature conditions associated with the observation. A brief review is given on DAC experiments in studying the melting temperature of iron at high pressures. The effect of light elements on the melting temperature is discussed in the end.

For more details on this topic, the following review articles are suggested.

1. Jephcoat, A.P., and S.P. Besedin, Temperature measurement and melting determination in the laser-heated diamond-anvil cell, *Phil. Trans. R. Soc. Lond. A*, *354* (1711), 1333-1360, 1996.
2. Shen, G., and D.L. Heinz, High pressure melting of deep mantle and core materials, in *Ultra High Pressure Mineralogy: Physics and Chemistry of the Earth's Deep Interior*, edited by R.J. Hemley, pp. 369-396, Mineralogical Society of America, Washington DC, 1998.
3. Boehler, R., High pressure experiments and the phase diagram of lower mantle and core materials, *Rev. Geophysics*, *38*, 221-245, 2000.

Diamond cell technique

Diamond as anvil and window

Diamond is a premier anvil material because it is the hardest material known, and it is transparent from infrared to hard x-rays, thus providing a window for probing samples by various methods and for heating samples by lasers. With the DAC technique, pressures beyond that at the center of the Earth have been reported [1]. The principal

components of a DAC are two opposing diamond anvils with a gasket in between. A drilled hole in the center of the gasket serves as sample chamber. For melting experiments at very high pressures, typical dimensions of a sample chamber are 10-20 μm thick and ~50 μm in diameter.

Heating diamond anvil cells

An easy way to provide heating is to heat the entire DAC externally. However, there is a temperature limit of ~1500 K with this method. To generate extreme high temperatures to melt iron at high pressures, internally heating methods are generally employed. One is the resistive wire heating, in which iron is used as a conductor wire and heating is applied electrically [2]. With this method, temperatures can go as high as its melting point, but pressures are limited because of deformation of the electrical leads as pressure increases. The other is the laser heating technique, in which near- or mid-infrared lasers (Nd:YAG, Nd:YLF, CO_2) are used for heating samples in DAC. There are, in principle, no pressure and temperature limitations associated with this technique. The challenge is to control pressure and temperature conditions, to measure them accurately, and to characterize the sample at defined conditions. A typical sample configuration is shown in Figure 1.

Pressure measurement

Pressures in the laser heated DAC are often measured by the ruby fluorescence method [3] before and after laser heating or during heating from unheated ruby chips away from the heating area. When the laser heating experiment is coupled with synchrotron radiation, pressures are estimated by measuring unit cell volumes of samples whose pressure-temperature-volume equations of state are known. For pressures measured before and after laser heating, thermal pressure (caused by the material's thermal expansion) has to be considered in estimating pressures at high temperature. Thermal pressure may be minimized by choosing a hydrostatic pressure medium and a small sample-to-medium ratio, and/or characterized with the use of highly collimated synchrotron radiation.

Temperature measurement

Temperature measurement is based on the collected radiation from thermal emission through the Planck radiation law: $I_\lambda = c_1\varepsilon(\lambda)\lambda^{-5}/[\exp(c_2/\lambda T)-1]$, where I_λ is spectral intensity, λ is wavelength, T is temperature, $c_1=2\pi hc^2=3.7418\text{x}10^{-16}$ Wm^2, $c_2=hc/k=0.014388$ mK, and $\varepsilon(\lambda)$ is emissivity with $\varepsilon(\lambda)=1$ for a blackbody. This method covering a range of wavelengths is often called *spectral radiometry*, as compared to the general pyrometry in which thermal radiation at only one wavelength is measured. One major advantage of spectral radiometry is that, assuming wavelength-independent emissivity, temperatures can be measured independently from the absolute emissivity. However, emissivity is often found to be wavelength dependent. Use of the available data on the wavelength-dependent emissivity at ambient pressure [4] gives about a 5% temperature correction downward at 3000 K and about 12% downward at 5000 K when compared with the results from the assumption of wavelength-independent emissivity. Unfortunately, such a correction cannot be accurately made because the wavelength dependence of emissivity is not currently known at high pressures and high temperatures**,**

and it can be strongly dependent on the surface finish of a DAC sample. This is the main limitation in the absolute accuracy of temperature measurement by the spectral radiometry method.

Melting criteria

Melting is thermodynamically defined as equilibrium between a solid and a liquid. When materials melt, their physical properties, such as density, viscosity, absorption properties, and electrical resistance, undergo a sudden change. Such property changes are characteristic for a first order phase transition and are often used for recognition of melting. Unlike other first order phase transitions, melting is characterized by the loss of long-range order and resistance to shear. To definitively identify melting, both of these two characteristics should be documented. Visual optical observation is a common way to determine whether melting has taken place. It is obvious that fluid flow observation is a good measure of the loss of resistance to shear. Therefore it has been widely used by almost all groups in the world [5,6]. However, visual observation (fluid flow) is less obvious as pressure increases, making it difficult to unambiguously define the onset of melting. Synchrotron x-ray diffraction has been combined with laser heated DAC and used for melting studies to document the loss of long range order upon melting. Melting at high pressure was identified by the appearance of diffuse scattering from the melt with the simultaneous loss of crystalline diffraction signals [7].

Synchrotron Mössbauer spectroscopy (SMS) provides another promising method to identify melting. SMS measures the atomic thermal displacement that can be used for documenting rigidity of a material. Upon melting the strong elastic resonance signal diminishes in SMS. The mean square thermal displacement of atoms (Lamb-Mössbauer factor) can be measured as a function of temperature, providing a plot for determining the onset of melting. Since measurement of SMS takes only a few seconds to minutes, it holds a great potential for high pressure melting studies.

Melting of core material at high pressures

Iron

Iron is the major component of the core. Knowledge of the melting curve of iron can constrain the temperature of the inner core boundary and anchor the Earth's temperature profiles. At pressures below 50 GPa, the phase diagram of iron is reasonably well known (Fig. 2). At ambient pressure, the stable phase is α-Fe with a body-centered cubic (bcc) structure. At high pressure it transforms to ε-Fe with hexagonal-close-packed (hcp) structure. At high temperature there is a large stability field for γ-Fe with face-centered-cubic (fcc) structure. Although a controversial new solid phase (called β-Fe) was reported [8], the existence of this phase was not confirmed in latter experiments [9,10]. For the melting curve, there is a converging consensus at pressures below 60 GPa, reflected by a narrow uncertainty range in Fig. 2. As pressure increases, uncertainties in phase boundaries, including the melting curve, become large as shown by wide bands in Fig. 2. The width of the bands represents the scatter in literature data from recent years. Factors causing these uncertainties include those in pressure determinations (neglecting thermal pressure, different equations of state and/or different standard materials), in temperature determinations (large temperature gradient and temporal variation, chromatic

aberration in optics), and in sample characterizations (different melting criteria, transition kinetics).

Uncertainties in the melting curve and the γ-ε transition lead to significant variations in the location of γ-ε-*liquid* triple point. Knowledge of its location is important because it is the starting point used for extrapolation the melting curve of ε-Fe to core pressures. As shown in Figure 2, the slope of γ-ε transition ranges from 25 to 40 K/GPa, placing the triple point between 60 GPa and 100 GPa. Such large uncertainties in the slope of the γ-ε transition mainly arise from the coexisting nature of these two phases in the pressure-temperature range, causing difficulties in identifying the boundary. The uncertainties are also contributed by the pressure-temperature determination associated with the use of different standard materials and/or different equations of state.

The melting data for iron above the triple point are scarce and scattered, reflecting the difficulty level of such experiment. It appears that the early DAC data [6,11] represent a lower bound of the melting curve in this region. The later experimental data falls at higher melting temperatures [9]. The shock wave data [12,13] lie close to the upper bound. Extrapolating the data to the inner core boundary, the melting temperature of iron is between 4800 K to 6000 K at 330 GPa.

Effects of light elements

As shown by Birch [14], the density of the earth's outer core is about ten percent too low to be pure iron, so the core must also contain some light elements. At present, there is no consensus on the dominant light element in the core.

At ambient pressure, the addition of a small amount of light elements decreases the melting temperature of iron by up to a few hundred degrees. Data at high pressure are scarce and limited in the Fe-FeO-FeS system [15,16]. Eutectic melting was found in the Fe-FeS system, while a solid solution mechanism was suggested for Fe-FeO system [16]. Boehler [17] pointed out that the melting curves in the Fe-FeS-FeO system converge to that of pure iron instead of diverge with increasing pressure.

However, several difficulties need to be addressed and overcome in melting experiments of multi-component systems using DAC. The laser heating spot could be on a scale similar to non-uniform samples, which could cause large experimental errors. Large temperature gradients in radial and axial directions could lead to compositional gradients (e.g., Soret diffusion), causing incomplete mixing during heating and melting. Significant developments are thus needed for constraints of light element effects on the melting temperature of iron.

References

[1] J. Xu, H. K. Mao, and P. M. Bell, Science **232**, 1404 (1986).

[2] R. Boehler, Geophy. Res. Lett. **13**, 1153 (1986); H. K. Mao, P. M. Bell, and C. Hadidiacos, in *High Pressure Research in Mineral Physics*, edited by M. H. Manghnani and Y. Syono (Terra Scientific Publishing Company/American Geophysical Union, Tokyo, Washington DC, 1987), pp. 135.

[3] H. K. Mao, J. Xu, and P. M. Bell, J. Geophys. Res. **91**, 4673 (1986).

[4] J. C. de Vos, Physica **20**, 690 (1954).

[5] R. Boehler, Rev. Geophysics **38**, 221 (2000); A. P. Jephcoat and S. P. Besedin, Phil. Trans. R. Soc. Lond. A **354** (1711), 1333 (1996); R. Jeanloz and A. Kavner, Phil. Trans. R. Soc. Lond. A **354** (1711), 1279 (1996).
[6] S. K. Saxena, G. Shen, and P. Lazor, Science **264**, 405 (1994).
[7] G. Shen, V. B. Prakapenka, M. L. Rivers et al., Phys. Rev. Lett. **92**, 185701 (2004).
[8] S. K. Saxena, L. S. Dubrovinsky, and P. Haggkvist, Geophys. Res. Lett **23**, 2441 (1995); D. Andrault, G. Fiquet, M. Kunz et al., Science **278** (5339), 831 (1997); L. S. Dubrovinsky, S. K. Saxena, and P. Lazor, Eur. J. Minerl. **10**, 43 (1998).
[9] Guoyin. Shen, H. K. Mao, R. J. Hemley et al., Geophy. Res. Lett. **25**, 373 (1998); Y. Z. Ma, M. Somayazulu, H. K. Mao et al., Phys. Earth Planet. Inter. **144**, 455 (2004).
[10] A. Kubo, E. Ito, T. Katsura et al., PEPI **this volume** (2003).
[11] R. Boehler, Nature **363**, 534 (1993).
[12] J. M. Brown and R. G. McQueen, J. Geophys. Res **91**, 7485 (1986).
[13] J. H. Nguyen and N. C. Holmes, Nature **427**, 339 (2004).
[14] F. Birch, J. Geophys. Res. **57**, 227 (1952).
[15] T. M. Usselmann, Am. J. Sci. **275**, 278 (1975); S. Urakawa, M. Kato, and M. Kumazawa, in *High pressure research in Mineral Physics*, edited by M. H. Manghnani and Y. Syono (Terra, Tokyo, 1987), pp. 95; A. E. Ringwood and W. Hibberson, Phys. Chem. Mineral. **17**, 313 (1990); Q. Williams, E. Knittle, and R. Jeanloz, J. Geophys. Res. **96**, 2171 (1991); Y. Fei, C. M. Bertka, and L. W. Finger, Science **275**, 1621 (1997).
[16] E. Knittle and R. Jeanloz, J. Geophys. Res. **96**, 16169 (1991); R. Boehler, Earth Planet. Sci. Lett. **111**, 217 (1992).
[17] R. Boehler, Phil. Trans. R. Soc. Lond. A **354**, 1265 (1996).
[18] T. J. Ahrens, K. G. Holland, and G. Q. Chen, Geophys. Res. Lett. **29** (7), 10.1029/2001GL014350 (2002).

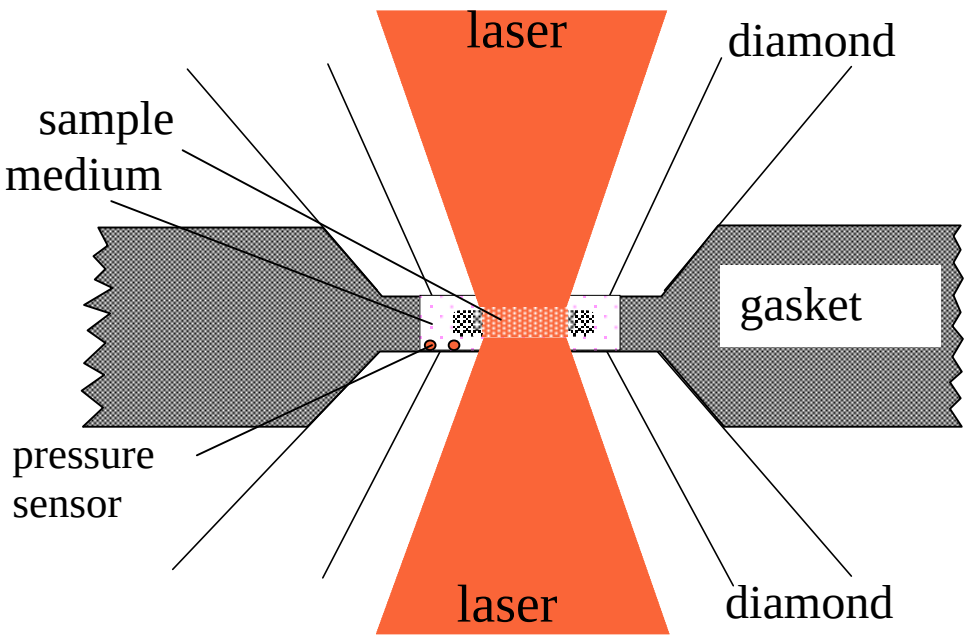

Figure 1. A typical sample configuration in laser heated diamond anvil cell experiment.

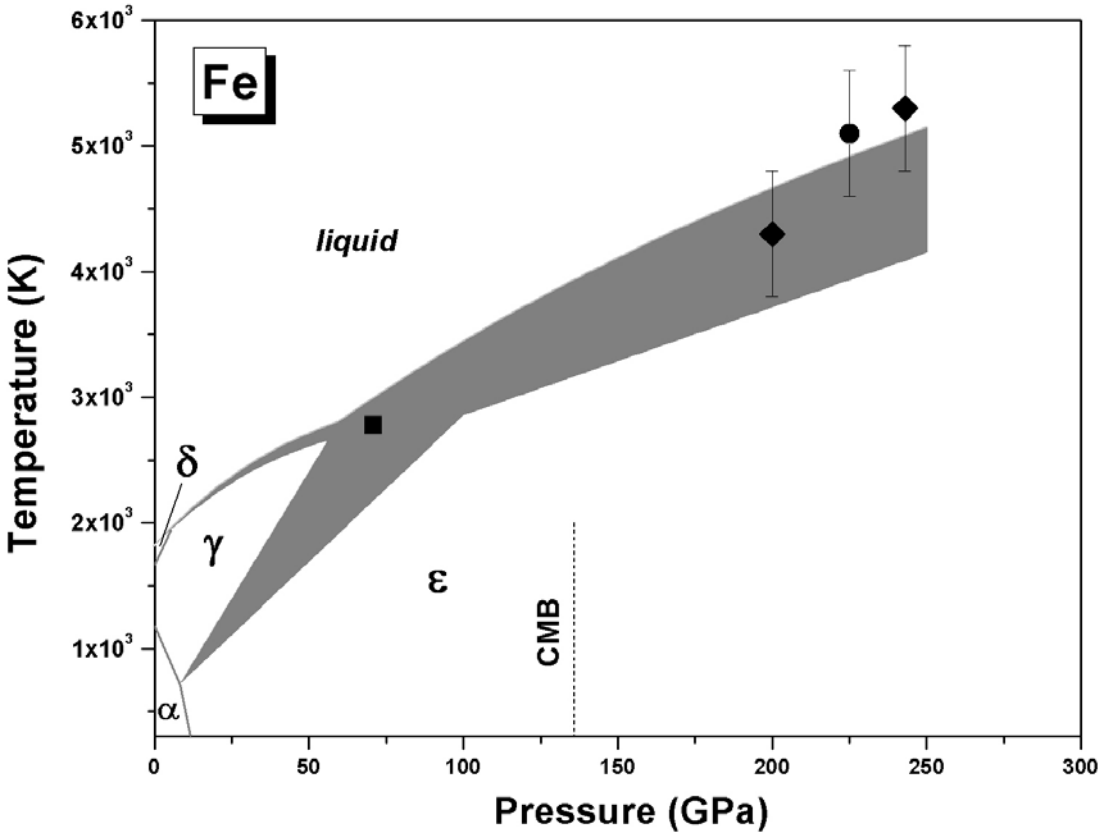

Figure 2. Iron phase diagram. Shaded areas represent the range of literature values in recent years with static diamond anvil cell experiments. Symbols are shock-wave data: square – Ahrens et al [18], diamonds – Brown and McQueen [12], circle – Nyuyen and Holmes [13]. Brown and McQueen's point at 200 GPa was interpreted as a solid-solid transition. All other points are referred as melting.